Designing Tapered Holey Fibers for Soliton Compression

Ming-Leung V. Tse, Peter Horak, Francesco Poletti, and David J. Richardson

***Abstract*—We investigate numerically the compression of femtosecond solitons at 1.55-μm wavelength propagating in holey fibers which exhibit simultaneously decreasing dispersion and effective mode area. We determine optimal values of holey fiber parameters and fiber lengths for soliton compression in the adiabatic and nonadiabatic regimes. Compression factors in excess of ten are found for fibers as short as a few meters.**

***Index Terms*—Fiber design and fabrication, microstructure optical fibers, pulse compression methods.**

I. Introduction

COMPRESSION of soliton pulses propagating in conventional dispersion decreasing optical fibers (DDF) is a well-established technique [1]. Early demonstrations at a wavelength of 1.55 μm already showed compression from 630 to 115 fs in a 100-m DDF and from 3.5 down to 230 fs in a 1.6-km DDF [2]. Pulse compression of higher order solitons in DDF with factors greater than 50 was also demonstrated [3]. The effect of the dispersion profile along the fiber on the performance of pulse compression in DDF was systematically investigated in [4] and the effects of higher order dispersion in [5]. A variant of the scheme using dispersion-decreasing fiber in a nonlinear optical loop mirror has been proposed for the compression of longer (picosecond) pulses [6].

Microstructured holey fibers offer the flexibility to extend adiabatic soliton compression to a much wider range of wavelengths and pulse energies than accessible with conventional optical fibers [7]. First, the large refractive index contrast between fiber core and cladding possible in holey fibers leads to large waveguide dispersion which can be used to compensate for the normal material dispersion at wavelengths below ~ 1.3 μm in silica fibers. Anomalous dispersion and hence soliton propagation can be easily achieved, for example, at 1.06 μm where efficient Yb-doped fiber laser sources exist [8]. Second, because of the small core size and thus high nonlinearity possible within holey fibers, compression already occurs at very low soliton energies and over short lengths of fiber. Compression of femtosecond solitons with pico-Joule energies at 1.06 μm has recently been demonstrated [9]. Finally, in contrast to conventional fibers, holey fibers can be fabricated where both dispersion *and* effective mode area decrease significantly, leading to enhanced compression factors. Dispersion- and mode-area decreasing holey fibers (DMDHFs) can be fabricated by varying the drawing conditions during the fiber draw, which in general allows for variation of fiber parameters on a length scale as short as 10 m [10]. For faster parameter variations along shorter lengths of fiber, a holey fiber has to be tapered on a specialized rig similarly to fibers fabricated for supercontinuum generation at short wavelengths [11]–[14].

In this paper, we investigate in detail the idea of using DMDHFs for fundamental soliton compression. The paper is organized as follows. In Section II, we analyze holey fiber dispersion and effective mode area versus fiber design parameters and the resulting soliton compression in DMDHFs under fully adiabatic conditions. In Section III, we compare these theoretical results with numerical simulations taking into account a variety of nonlinear effects and higher order dispersion. Section IV investigates the compression factor for different fiber lengths and discusses the minimum length required for near-adiabatic conditions. In Section V, nonadiabatic compression in short lengths of DMDHFs is discussed. Section VI deals with the important issues of fiber loss and fiber fabrication. Finally, we summarize our results in Section VII.

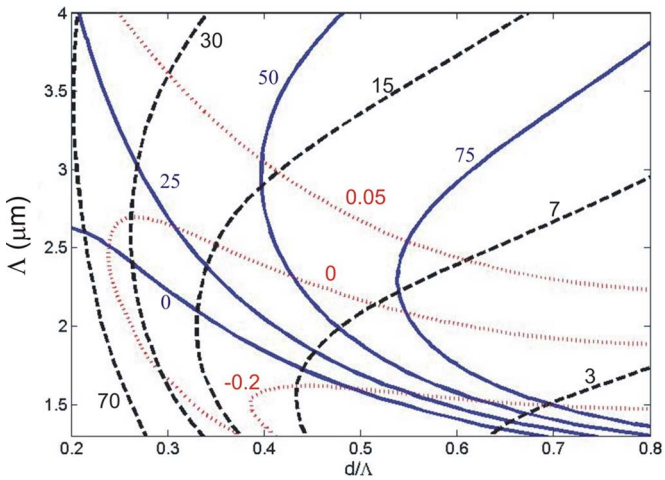

Fig. 1. Contour map for dispersion [solid line; units of ps/(nm km)], dispersion slope[(dotted line; ps/(nm^{2}km)] and effective area [dashed line; μm^2] versus pitch Λ and d/Λ for holey fibers of hexagonal geometry at 1.55-μm wavelength.

II. Holey Fiber Design and Ideal Adiabatic Compression

We present in Fig. 1 the dependence of dispersion D, dispersion slope D_s, and effective mode area A_{eff} on hole-to-hole spacing Λ and air-filling fraction d/Λ of holey fibers with regular hexagonal geometry at 1.55 μm. The map has been calculated by simulating a number of fibers on a regular $(d/\Lambda, \Lambda)$

Manuscript received February 21, 2007; revised July 25, 2007.

The authors are with the Optoelectronics Research Centre, University of Southampton, Southampton SO17 1BJ, U.K. (e-mail: mlt@orc.soton.ac.uk).

Color versions of one or more of the figures in this paper are available online at http://ieeexplore.ieee.org.

Digital Object Identifier 10.1109/JQE.2007.910446

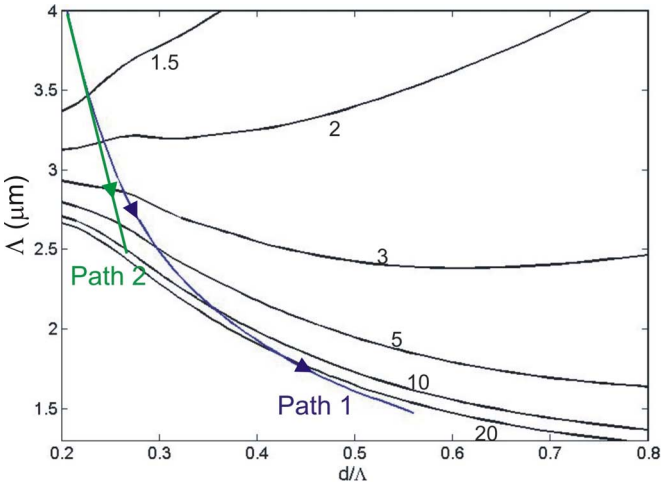

Fig. 2. Contour map for adiabatic compression factors corresponding to Fig. 1.

grid with a full vector finite element method solver and by applying a subsequent 2-D spline to create smooth contours. The choice of a dense enough grid of 17×13 points ensures that the accuracy of each point on the map is equal or better than the accuracy practically achievable during the fiber fabrication. The map was obtained for fibers with 8 rings of air-holes; however it was found that in the design region of interest for this study both D and A_{eff} are not significantly affected by an increase in the number of rings. By appropriate fiber fabrication and/or tapering a large variation of both D and A_{eff} can be achieved along the length of a single fiber. In this paper we are concerned with optimizing the corresponding rate of parameter change along the fiber with respect to soliton compression.

For given fiber parameters and pulse energy E_{sol}, the full width at half maximum (FWHM) of a fundamental soliton is [15]

$$\tau = 1.76 \frac{\lambda^3 D A_{\text{eff}}}{2\pi^2 c n_2 E_{\text{sol}}} \tag{1}$$

where λ is the wavelength and n_2 is the nonlinear-index coefficient. In the idealized case of a lossless fiber and an arbitrarily slow change of D and A_{eff} along the fiber, E_{sol} stays constant, the pulse compression is adiabatic, and therefore the pulsewidth is proportional to the product DA_{eff}. In real fibers however, fiber loss, the delayed nonlinear Raman response, and higher order dispersion affect the soliton propagation and achievable compression. These effects will be discussed in Sections III–VI, but are neglected here.

Based on (1), we obtain the contour map of the adiabatic compression factor, Fig. 2, corresponding to the map of fiber parameters in Fig. 1. Fig. 2 is normalized to the top left corner of the figure which has the largest value of DA_{eff}. A tapered fiber with parameters changing from that point to any other point on the map will result in compression of a soliton at 1.55 μm by the factor shown in the figure, provided that changes of fiber parameters over one local dispersion length are small. We note that compression factors of 20 and higher are possible in theory, if the end point of the holey fiber is close to the zero-dispersion line of Fig. 1.

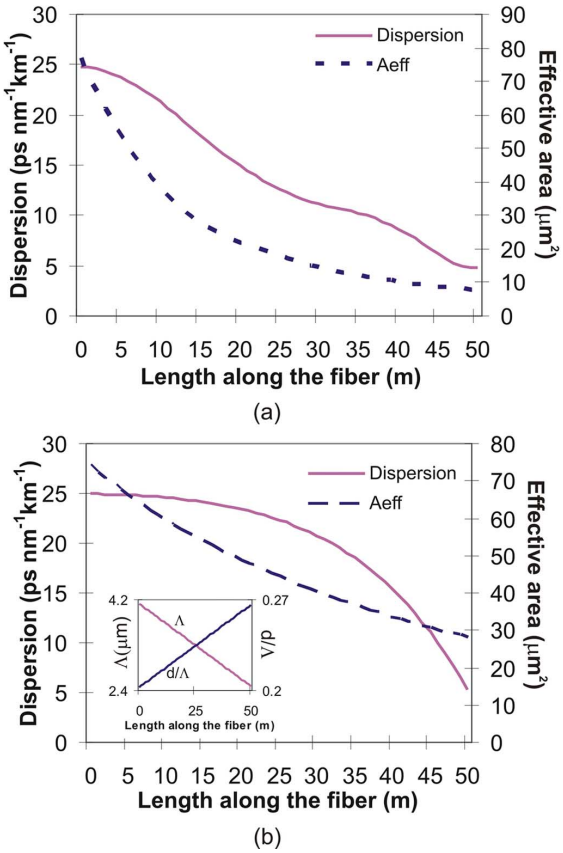

Fig. 3. Dispersion and effective area profiles along a 50-m fiber for (a) Path 1 and (b) Path 2 of Fig. 2. Inset: In both cases the fiber parameters Λ and d/Λ vary linearly along the fiber from $(d/\Lambda = 0.20, \Lambda = 4.12)$ to $(d/\Lambda = 0.27, \Lambda = 2.48)$.

III. Adiabatic Compression in Long Fibers

For a more detailed investigation, we performed numerical simulations of the generalized nonlinear Schrödinger equation using a standard split-step Fourier tool, which takes into account higher order dispersion as well as nonlinear Kerr and Raman effects. This is done for fibers with parameters following different paths on the contour map, two of the paths are shown in Fig. 2. Fiber loss is neglected in the following, but will be discussed later in Section VI. Furthermore, we assume input solitons of 400 fs duration, which on one hand provides a short dispersion length of $L_D \sim 5$ m such that fiber propagation losses are small over this scale, but which on the other hand is long enough to avoid excessive spectral bandwidths.

In this section, we analyze pulse compression in DMDHFs of 50 m length, which is long compared to $L_D \sim 5$ m, and fiber parameters in the top left corner of Fig. 1. First, we choose a path in Fig. 1 that gives a large decrease of dispersion *and* mode area, while the fiber remains both single mode and in the anomalous dispersion regime. This is indicated as Path 1 in Fig. 2. Here, D is decreasing by a factor of ~ 5 and A_{eff} is decreasing by a factor of ~ 10 from the top left corner of the map to a point close to $D = 0$. The profiles of D and A_{eff} along the length of the fiber are shown in Fig. 3(a).

The simulated FWHM for Path 1 is shown in Fig. 4. While we would expect adiabatic compression for these parameters, we observe that after ~ 20 m of fiber the width deviates from that

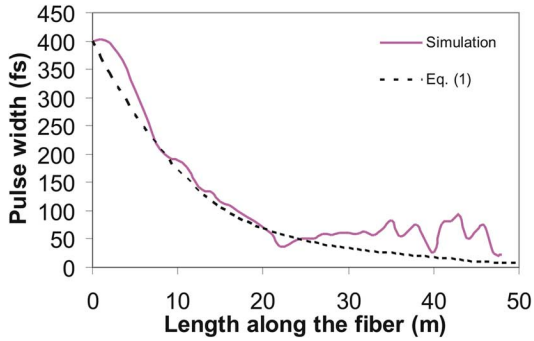

Fig. 4. Simulated pulsewidth (FWHM) in the fiber with dispersion and effective area profiles along Path 1.

found by the analytic expression (1). A closer analysis reveals that two effects prevent further compression at this point.

Firstly, the dispersion slope decreases from 0.046 to -0.267 ps/(nm^{2}km) along the fiber. Thus, during the second half of the fiber the zero-dispersion wavelength shifts continuously toward the soliton. When the zero-dispersion wavelength is found close to the soliton wavelength, the soliton starts to shed energy into dispersive waves [16]. This effect is clearly observed in the simulated spectra at different positions along the fiber shown in Fig. 5(a). The first dispersive wave appears at ~ 2–μm wavelength after 23 m of propagation. Subsequently more new components are generated below 2 μm as the zero-dispersion wavelength continues to move to shorter wavelengths. Note that this problem can be avoided with longer input pulses of e.g., 1 or 2 ps which lead to smaller output bandwidths. However, a much longer fiber with very low loss is needed in this case for adiabatic compression as the dispersion length is of the order of tens of meters.

Secondly, the large decrease in A_{eff} and the corresponding increase in the nonlinearity lead to temporal broadening by Raman soliton self-frequency shifting (SSFS) [17]. This effect is clearly observed in the spectra, Fig. 5(b). Note that for this particular simulation we kept $D_s = 0$ through out the fiber.

These results impose certain restrictions on fiber parameters which lead to high soliton compression factors. First, the fiber should have an end point near the crossing point of the line of zero dispersion $D = 0$ and the line of zero dispersion slope $D_s = 0$ [18] to avoid the resonant generation of dispersive waves. Second, the effective area A_{eff} can only be reduced by a certain fraction to reduce SSFS. For D and A_{eff} to be either constant or decreasing along the fiber, holey fiber parameters must therefore be chosen in the top left area of the map in Fig, 1. Path 2 of Fig. 2 represents such a choice. Here, D decreases by a factor of ~ 5 [from 25 to 5 ps/(nm km)] and A_{eff} by a factor of ~ 2.5 (from 75 to 30 μm^2) along the fiber, the corresponding profiles are shown in Fig. 3(b). The simulated pulsewidth in this case is shown in Fig. 6. We now find excellent agreement with the analytic approximation (1), which suggests that the soliton compression is indeed adiabatic. A small SSFS is still observed in the corresponding spectrum but no dispersive waves are generated. A 400-fs soliton pulse is compressed down to 33 fs, a compression factor of ~ 12. The adiabaticity of the soliton compression is further confirmed by the fact that simulations using

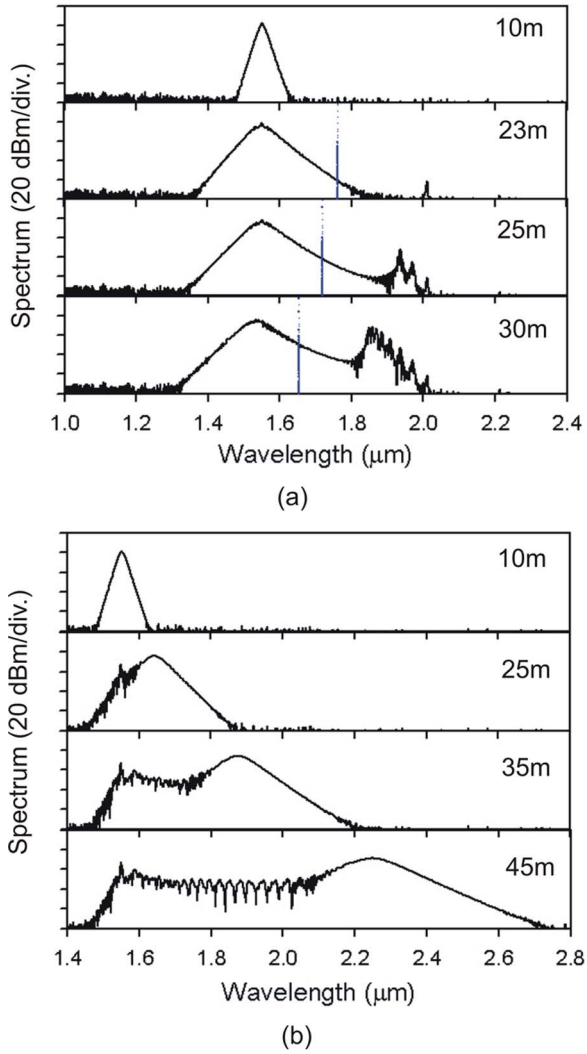

Fig. 5. Simulated spectra at different distances along the fiber (Path 1) (a) showing the effects of dispersion slope when Raman effects are neglected in the simulation (dotted lines indicate zero dispersion wavelengths) and (b) showing the effects of Raman shifting when $D_s = 0$ for the entire length.

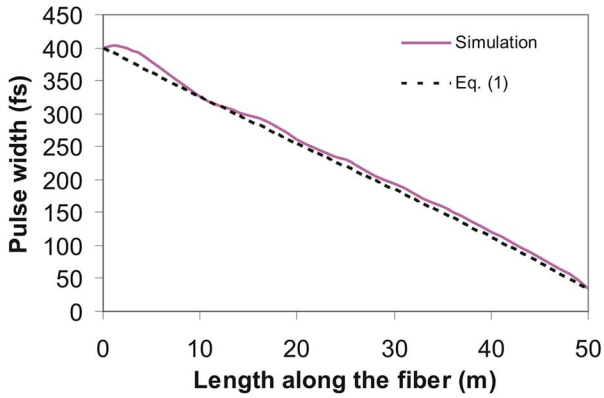

Fig. 6. Simulated pulsewidth (FWHM) in the fiber with dispersion and effective area profiles along Path 2.

paths with the same start and end points as Path 2 but alternative routes in between yield very similar performances. Finally, we fitted a soliton intensity profile to the simulated output. This yielded a perfect fit with as little as 0.04% of the output energy lost from the soliton during compression.

IV. Minimized Fiber Length for Adiabatic Compression

In this section, we investigate the minimum fiber length necessary to achieve high compressions. We study fibers down to a few meters in length which could potentially be fabricated in a holey fiber tapering rig.

We use again the fiber parameters found in Path 2 of Fig. 2, but now we investigate different lengths of fiber and allow for nonuniform changes of Λ and d/Λ along the fiber, that is, different profiles of D and A_{eff} [4]. Our simulations indicate that the shortest fiber length over which the maximum compression can be achieved requires constant effective gain g_{eff} along the fiber [19], [20]. In its dimensionless form, this condition can be written as

$$g_{\text{eff}} = -\tau_0^2 \frac{2\pi c}{\lambda^2 D}\left(\frac{1}{2D}\frac{\partial D}{\partial z_{\text{opt}}} + \frac{1}{2A_{\text{eff}}}\frac{\partial A_{\text{eff}}}{\partial z_{\text{opt}}}\right) = \text{const} \quad (2)$$

where τ_0 is the initial soliton width and z_{opt} is the position along the optimized fiber. Since the parameter pair $(\Lambda, d/\Lambda)$ should follow the same path (Path 2) in the contour map, z_{opt} can be mapped onto the position z of Fig. 3 by a function $z_{\text{opt}}(z)$. For every constant value of g_{eff}, (2) then provides a differential equation for $z_{\text{opt}}(z)$, whose solution is the optimized profile for a fiber length $L(g_{\text{eff}})$. As an example, Fig. 7(a) shows the optimized D and A_{eff} profiles for a 15-m fiber. Fig. 7(b) depicts the corresponding simulated pulsewidth together with the prediction by (1), showing that a compression factor of 12 can still be achieved with this fiber. In this case, the output was well fitted by a soliton and a pedestal containing 7.8% of the energy.

We used the same optimization routine for different lengths of fiber and plot the simulated output pulsewidth in Fig. 8 together with results obtained for non-optimized profiles where Λ and d/Λ vary linearly along the fiber. As expected, no difference is found for long fiber lengths where both profiles are adiabatic everywhere along the fiber, however there exist marked differences for fibers less than 5 m long. We found that a compression factor of 10 can still be achieved over a length of 5 m which is close to the dispersion length. For shorter lengths, only the optimized profiles lead to similar compression factors. However the oscillatory behavior of the output pulsewidth with fiber length indicates that pulse compression is no longer fully adiabatic in this regime.

V. Nonadiabatic Compression in Short Fibers

Significant compression can still be observed for DMDHFs shorter than 5 m in the nonadiabatic regime [21]. As an example, we simulated the pulse propagation over only 2 m of fiber with the start and end points of Path 2, but not necessarily following a direct route. The top left region of the map (Fig. 1) is again shown in Fig. 9(a). Two new paths are indicated with the same end points as Path 2. Path 3 consists of a first part where A_{eff} is constant and only D is decreasing, and a second part where A_{eff} is decreasing at constant D. Path 4 exhibits the opposite behavior. The corresponding pulse compression is shown in Fig. 9(b), together with the results of a 5-m near-adiabatic compression as discussed in the previous section. For the short 2 m fiber, achievable compression varies significantly among different paths. The shortest pulses are found for Path 4 where A_{eff} is decreased first and D later. In this case, compression of

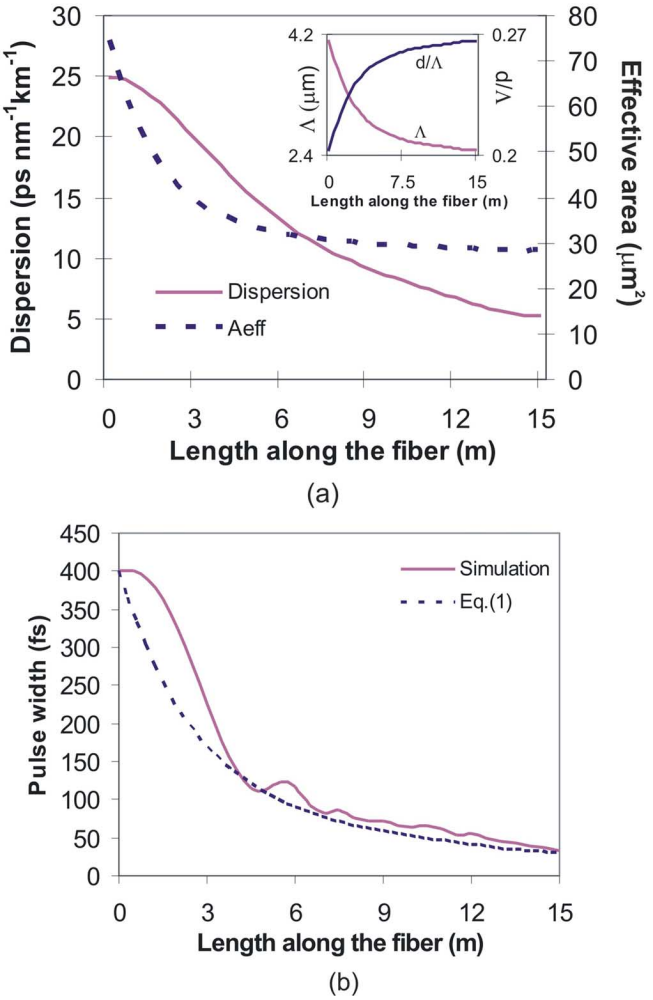

Fig. 7. (a) Optimized D and A_{eff} profiles for a 15-m fiber following path 2 using the constant effective gain method. Inset: the variation of Λ and d/Λ along the fiber. (b) Simulated pulsewidths (FWHM) in the fiber with the optimized dispersion and effective area profiles.

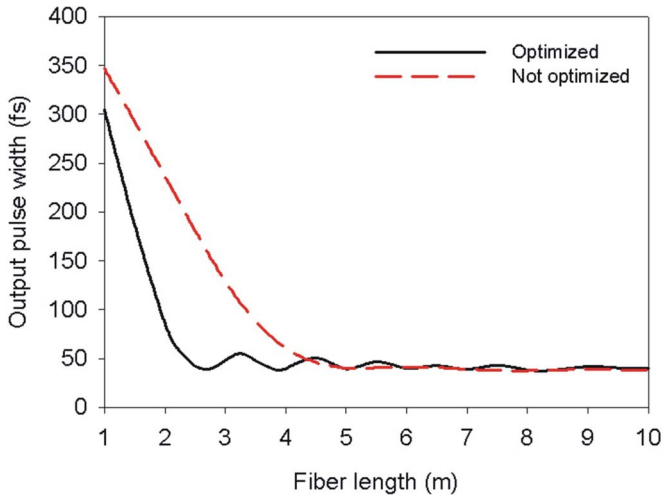

Fig. 8. Output pulsewidth for a 400-fs soliton input for fibers of different lengths following Path 2 with and without the constant effective gain (optimized) method.

400-fs pulses down to 65 fs is observed, a compression factor of ~ 6 compared to a factor of 10 for a 5-m fiber and a factor

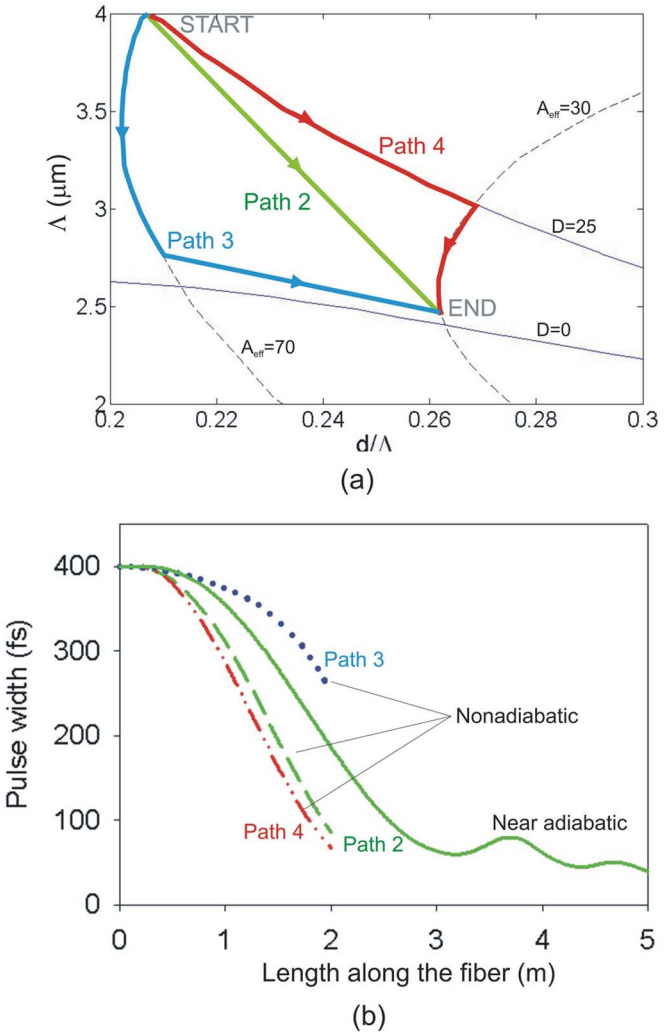

Fig. 9. (a) Contour map for effective area (μm^2) and dispersion (ps/(nm km)) versus Λ and d/Λ for holey fibers of hexagonal geometry at 1.55-μm wavelength showing Paths 2–4. (b) Pulse width along these paths under optimized near-adiabatic (5-m fiber length) and nonadiabatic (2-m fiber length) conditions.

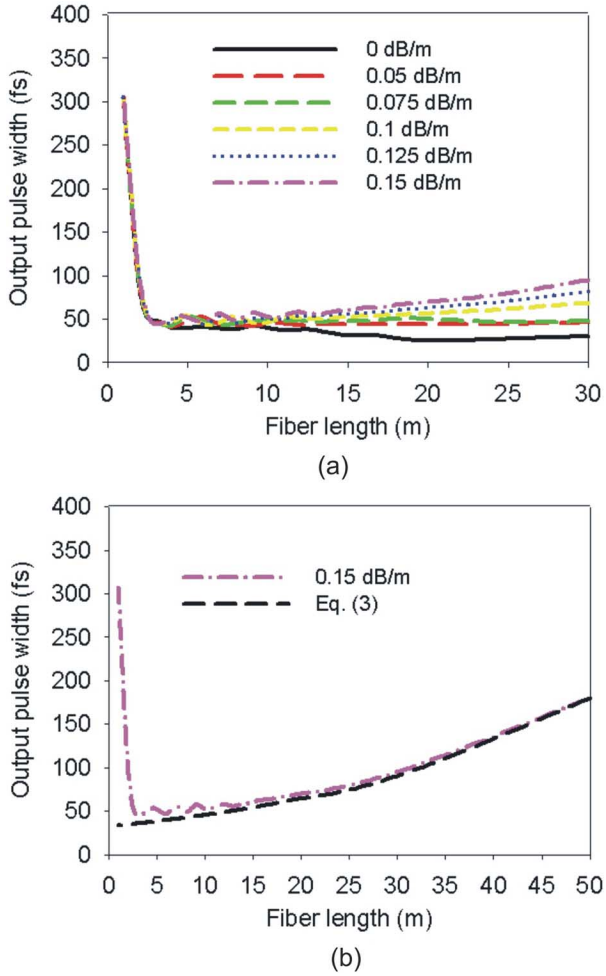

Fig. 10. Simulated output pulsewidth for fibers with D and A_{eff} profiles similar to Fig. 7(a) for (a) different fiber lengths and losses, (b) different fiber length and loss $= 0.15$ dB/m, and the calculated pulsewidth using (3).

of 12 for 15 m. By contrast, Path 3 only gives rise to a minor compression by less than a factor of two. We explain this large difference in performance as follows. A soliton is commonly interpreted as a pulse where the broadening effect of dispersion is exactly compensated by the focusing effect of the nonlinearity. For soliton compression we, therefore, expect the nonlinearity to play the major role and thus an initial decrease of the effective area (increase of nonlinearity) will lead to faster compression, in agreement with our numerical results.

Fitting the output pulses in the nonadiabatic regime with soliton profiles revealed pedestals containing 29.8%, 6.8%, and 33.6% of the energy for paths 2, 3, and 4, respectively. As expected, this loss of energy is much larger than in the adiabatic regime. However, it was found that the output pulses were still better matched by a soliton profile than, for example, by a Gaussian pulse shape.

VI. Fiber Loss and Fiber Fabrication

In real fibers, soliton compression is limited by propagation losses. In this case, the soliton energy in (1) is not constant, but decreases exponentially with propagation length. The pulse width under ideal adiabatic conditions thus is given by

$$\tau = 1.76\frac{\lambda^3 D A_{\text{eff}}}{2\pi^2 c n_2 E_0 \exp(-\alpha L)} \tag{3}$$

where E_0 is the soliton energy at the input, α is the fiber loss and L is the length along the fiber. We introduced realistic propagation losses into our numerical simulations and investigated the best fiber design and length accordingly.

Let us again consider Path 2 with varying parameters Λ and d/Λ along the fiber and with the optimized D and A_{eff} profiles rescaled from Fig. 7(a) to various fiber lengths. The simulated output pulse widths for 400 fs soliton input for different fiber lengths and losses are shown in Fig. 10(a). The optimum length for the chosen profiles is between 3 and 10 m. For example, in the case of 0.15 dB/m fiber loss, the minimum output pulsewidth is 45 fs with a fiber length of ~ 3 m, see Fig. 10(b). We also observe that for long fibers the simulated output pulse widths agreed very well with the analytical prediction (3), where good adiabaticity is observed.

The fibers investigated in this paper so far require large d/Λ and small Λ, which leads to large confinement losses of the fundamental mode in such tapers [22], [23]. In order to reduce the

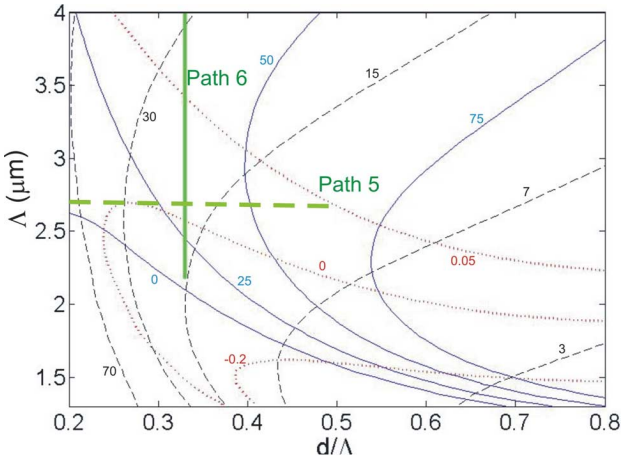

Fig. 11. Contour map for dispersion [solid line; units of ps/(nm km)], dispersion slope [dotted line; ps/(nm^{2}km)] and effective area [dashed line; μm^2] with paths that have either constant d/Λ or constant pitch.

confinement loss to an acceptable level, as many as 12–14 rings of identical holes are needed in this regime. One way to reduce the number of rings, and thus to facilitate fabrication, is to use larger hole sizes in the outer rings of the fiber structure. Our numerical mode calculations indicate that structures with 7 rings of holes with values for Λ and d/Λ as employed here and 2 outer rings of larger holes $(d/\Lambda > 0.8)$ exhibit similar dispersion profiles and thus should lead to similar pulse compression properties while significantly reducing confinement losses. We note, however, that the presence of different hole sizes may impede tapering of the fibers over the whole range of parameters required for efficient compression.

For any of the fibers investigated so far, both d/Λ and Λ are varying at the same time along the fiber, which requires accurate control of the air pressure in the holes and of the drawing temperature and speed during the fiber tapering process in order to achieve a specific parameter profile as, for example, shown in Fig. 7(a). This renders the fabrication of such fibers labor intensive and challenging. In practice, it may be desirable to find new paths in Fig. 1 for fibers which are more readily fabricated, even at the cost of slightly smaller compression ratios. Two possible scenarios are shown in Fig. 11. The first is to keep Λ constant and vary d/Λ,as indicated by Path 5, which can be achieved by varying the pressure in the air holes while simultaneously using fiber diameter feed back control during the fiber draw. However, fibers following such a path on the contour map have either D or A_{eff} decreasing but not both, which limits achievable compression factors. The second possibility for relatively easy fabrication of DMDHFs is to keep d/Λ constant and vary Λ such as shown by Path 6 in Fig. 11, which can be achieved by varying the fiber drawing speed.

Many paths with constant d/Λ offer the possibility of soliton compression, but most of the paths encounter the problems discussed above such as Raman SSFS, large third-order dispersion, or high losses. A good option is Path 6 with $d/\Lambda = 0.33$. Here, Λ decreases from 4 to 2.2 μm, D decreases from 40 to 8 ps/(nm km), and A_{eff} decreases from 30 to 15 μm^2, allowing for a compression factor of 10 in the adiabatic regime. Because of the large negative dispersion slope at the fiber end, compression of 400 fs

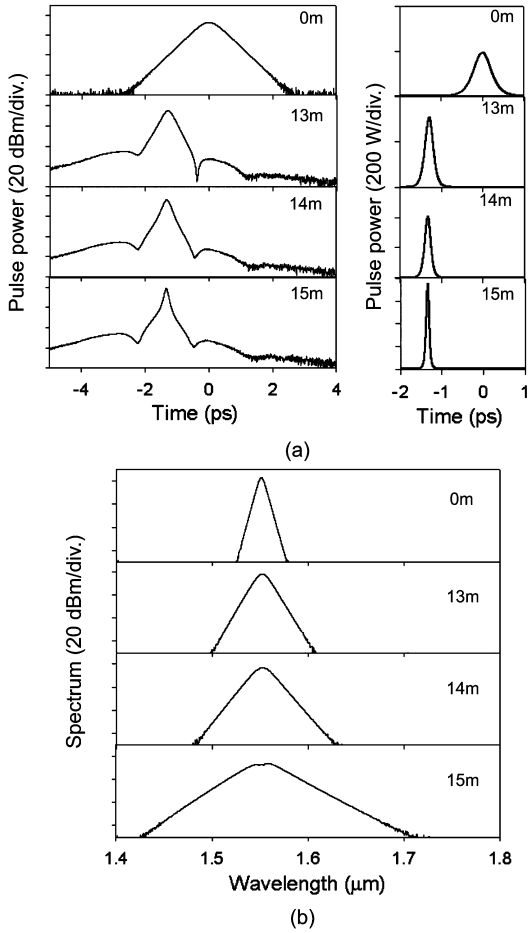

Fig. 12. Simulated (a) pulse shape (left: logarithmic scale; right: linear scale) and (b) spectrum for a fiber ($\text{loss} = 0.1$ dB/m) following Path 6 with a 500-fs soliton input at different positions along the fiber.

input solitons leads to some shedding of energy into dispersive waves, but a small increase of the input width to 500 fs reduces the output bandwidth sufficiently to avoid this problem. The resulting spectra and pulse shapes for a 15 m fiber with a loss of 0.1 dB/m are shown in Fig. 12. A compression factor of ~ 6 is found, with the output pulse maintaining high quality.

VII. Conclusion

We have investigated compression of femtosecond solitons in silica holey fibers of decreasing dispersion and effective mode area, which can be fabricated by changing the structural design parameters Λ and d/Λ during the fiber draw or by additional tapering. Long low-loss fibers with slowly changing parameters lead to adiabatic compression and the highest compression factors. In the presence of realistic fiber losses, it is essential to minimize the fiber length while maintaining high compression. We found that best compression over short fiber lengths is obtained in the adiabatic propagation regime if the effective gain is constant along the fiber. For even shorter fiber lengths compression is nonadiabatic but high compression factors can still be achieved by careful optimization of dispersion and effective mode area profiles along the fiber. A specific example of a fiber structure has been demonstrated which provides a compression factor of 12 in the adiabatic regime (>15 m of fiber), a factor

of 10 over 5 m under optimized near-adiabatic conditions, and a factor of 6 over 2 m of nonadiabatic compression. Finally, the effects of loss and the feasibility of fabrication has been investigated. A simple fabrication design has been proposed, where adiabatic compression by a factor of ~ 6 can be obtained for a fiber with a loss of 0.1 dB/m.

REFERENCES

[1] S. V. Chernikov and P. V. Mamyshev, "Femtosecond soliton propagation in fibers with slowly decreasing dispersion," *J. Opt. Soc. Amer. B*, vol. 8, pp. 1633–1641, 1991.

[2] S. V. Chernikov, E. M. Dianov, D. J. Richardson, and D. N. Payne, "Soliton pulse compression in dispersion-decreasing fiber," *Opt. Lett.*, vol. 18, pp. 476–478, 1993.

[3] M. D. Pelusi and H.-F. Liu, "Higher order soliton pulse compression in dispersion-decreasing optical fibers," *IEEE J. Quantum Electron.*, vol. 33, no. 3, pp. 1430–1439, Aug. 1997.

[4] A. Mostofi, H. Hatami-Hanza, and P. L. Chu, "Optimum dispersion profile for compression of fundamental solitons in dispersion decreasing fibers," *IEEE J. Quantum Electron.*, vol. 33, no. 4, pp. 620–628, Apr. 1997.

[5] K.-T. Chan and W.-H. Cao, "Enhanced compression of fundamental solitons in dispersion decreasing fibers due to the combined effects of negative third-order dispersion and Raman self-scattering," *Opt. Commun.*, vol. 184, pp. 463–474, 2000.

[6] P. K. A. Wai and W.-H. Cao, "Ultrashort soliton generation through higher order soliton compression in a nonlinear optical loop mirror constructed from dispersion-decreasing fiber," *J. Opt. Soc. Amer. B*, vol. 20, pp. 1346–1355, 2003.

[7] J. Hu, B. S. Marks, C. R. Menyuk, J. Kim, T. F. Carruthers, B. M. Wright, T. F. Taunay, and E. J. Friebele, "Pulse compression using a tapered microstructure optical fiber," *Opt. Exp.*, vol. 14, pp. 4026–4036, 2006.

[8] M. L. V. Tse, P. Horak, F. Poletti, N. G. R. Broderick, J. H. V. Price, J. R. Hayes, and D. J. Richardson, "Supercontinuum generation at 1.06 μm in holey fibers with dispersion flattened profiles," *Opt. Exp.*, vol. 14, pp. 4445–4451, 2006.

[9] M. L. V. Tse, P. Horak, J. H. V. Price, F. Poletti, F. He, and D. J. Richardson, "Pulse compression at 1.06 μm in dispersion-decreasing holey fibers," *Opt. Lett.*, vol. 31, pp. 3504–3506, 2006.

[10] A. Kudlinski, A. K. George, J. C. Knight, J. C. Travers, A. B. Rulkov, S. V. Popov, and J. R. Taylor, "Zero-dispersion wavelength decreasing photonic crystal fibers for ultraviolet-extended supercontinuum generation," *Opt. Exp.*, vol. 14, pp. 5715–5722, 2006.

[11] M. Foster, A. Gaeta, Q. Cao, and R. Trebino, "Soliton-effect compression of supercontinuum to few-cycle durations in photonic nanowires," *Opt. Exp.*, vol. 13, pp. 6848–6855, 2005.

[12] P. Falk, M. Frosz, and O. Bang, "Supercontinuum generation in a photonic crystal fiber with two zero-dispersion wavelengths tapered to normal dispersion at all wavelengths," *Opt. Expr.*, vol. 13, pp. 7535–7540, 2005.

[13] S. Leon-Saval, T. Birks, W. Wadsworth, P. S. J. Russell, and M. Mason, "Supercontinuum generation in submicron fiber waveguides," *Opt. Exp.*, vol. 12, pp. 2864–2869, 2004.

[14] J. M. Dudley, G. Genty, and S. Coen, "Supercontinuum generation in photonic crystal fiber," *Rev. Mod. Phys.*, vol. 78, pp. 1135–1184, 2006.

[15] G. P. Agrawal, *Nonlinear Fiber Optics*, 3rd ed. San Diego, CA: Academic, 2001.

[16] A. V. Husakou and J. Herrmann, "Supercontinuum generation of higher order solitons by fission in photonic crystal fibers," *Phys. Rev. Lett.*, vol. 87, pp. 203901/1–203901/4, 2001.

[17] F. M. Mitschke and L. F. Mollenauer, "Discovery of the soliton self-frequency shift," *Opt. Lett.*, vol. 11, pp. 659–661, 1986.

[18] K. R. Tamura and M. Nakazawa, "Femtosecond soliton generation over a 32 nm wavelength range using a dispersion-flattened dispersion-decreasing fiber," *IEEE Photon. Technol. Lett.*, vol. 11, no. 3, pp. 319–321, Mar. 1999.

[19] V. A. Bogatyrev, M. M. Bubnov, E. M. Dianov, A. S. Kurkov, P. V. Mamyshev, A. M. Prokhorov, S. D. Rumyantsev, V. A. Semenov, S. L. Semenov, A. A. Sysoliatin, S. V. Chemikov, A. N. Gur'yanov, G. G. Devyatykh, and S. I. Miroshnichenko, "A single-mode fiber with chromatic dispersion varying along the length," *J. Lightw. Technol.*, vol. 9, no. 5, pp. 561–566, May 1991.

[20] P. V. Mamyshev, S. V. Chernikov, and E. M. Dianov, "Generation of fundamental soliton trains for high-bit-rate optical fiber communication lines," *IEEE J. Quantum. Electron.*, vol. 27, no. 10, pp. 2347–2355, Oct. 1991.

[21] F. K. Katemi, "Analysis of nonadiabatically compressed pulses from dispersion-decreasing fiber," *Opt. Lett.*, vol. 27, pp. 1637–1639, 2002.

[22] H. C. Nguyen, B. T. Kuhlmey, M. J. Steel, C. L. Smith, E. C. Mägi, R. C. McPhedran, and B. J. Eggleton, "Leakage of the fundamental mode in photonic crystal fiber tapers," *Opt. Lett.*, vol. 30, pp. 1123–1125, 2005.

[23] S. Laflamme, S. Lacroix, J. Bures, and X. Daxhelet, "Understanding power leakage in tapered solid core microstructured fibers," *Opt. Exp.*, vol. 15, pp. 387–396, 2007.

Ming-Leung V. Tse was born in Hong Kong in 1979. He received the M.Sci. degree in theoretical physics from the University of St. Andrews, St. Andrews, U.K., in 2002, and the M.Sc. degree in photonics and optoelectronic devices, jointly from the University of St. Andrews and Heriot-Watt University, Edinburgh, U.K., in 2003. He joined the Optoelectronics Research Centre, University of Southampton, Southampton, U.K., in 2003 where he is currently pursuing the Ph.D. degree, working on the development of nonlinear holey fibers.

As part of his M.Sc. degree, he spent three months working at BAE Systems Advanced Technology Centre, Great Baddow, U.K.

Peter Horak received the M.Sc. degree in theoretical physics and the Ph.D. degree in theoretical quantum optics from the University of Innsbruck, Innsbruck, Austria, in 1993 and 1998, respectively.

He joined the Optoelectronics Research Centre, University of Southampton, Southampton, U.K., in 2001, where he is currently a Senior Research Fellow. His main research interest is in the theory and modeling of nonlinear and quantum optical phenomena and devices. His current research includes work on microresonators, holey fibers, nonlinear fiber optics, short-pulse propagation, and noise properties of optoelectronics devices.

Francesco Poletti received the Laurea degree in electronics engineering from the University of Parma, Parma, Italy, in 2000 and the Ph.D. degree in optoelectronics from the Optoelectronics Research Centre, University of Southampton, Southampton, U.K., in 2007.

His research interests include nonlinear optics, inverse design methods, numerical techniques for electromagnetic modelling, and the design and applications of index guiding and photonic bandgap guiding fibers.

David J. Richardson was born in Southampton, U.K., in 1964. He received the B.Sc. and Ph.D. degrees in fundamental physics from Sussex University, Sussex, U.K., in 1985 and 1989, respectively.

He joined the then recently formed Optoelectronics Research Centre (ORC), Southampton University, Southampton, U.K., as a Research Fellow in May 1989. He is now a Deputy Director of the ORC where he is responsible for Optical Fibre Device and Systems research. His current research interests include amongst others: microstructured fibers, high-power fiber lasers, short pulse lasers, optical fiber communications, and nonlinear fiber optics. He has published more than 600 conference and journal papers in his time at the ORC, and produced over 20 patents. He is a frequent invited speaker at the leading international optics conferences in the optical communications, laser and nonlinear optics fields and is an active member of both the national and international optics communities.

Prof. Richardson was awarded a Royal Society University Fellowship in 1991 in recognition of his pioneering work on short pulsed fiber lasers and was made a Fellow of the Optical Society of America in 2005.